

**RERTR 2009 _ 31st INTERNATIONAL MEETING ON
REDUCED ENRICHMENT FOR RESEARCH AND TEST REACTORS**

**November 1-5, 2009
Kempinski Hotel Beijing Lufthansa Center
Beijing, China**

**SEM CHARACTERIZATION OF AN IRRADIATED DISPERSION
FUEL PLATE WITH U-10MO PARTICLES AND 6061 AL MATRIX**

**D. D. KEISER, JR., J. F. JUE, A. B. ROBINSON, P. G. MEDVEDEV, AND M. R.
FINLAY¹**

*Nuclear Fuels and Materials Division, Idaho National Laboratory
P. O. Box 1625, Idaho Falls, Idaho 83403 USA*

*¹Australian Nuclear Science and Technology Organization
PMB 1, Menai, NSW, 2234,
Australia*

ABSTRACT

It has been observed that during irradiation of a dispersion fuel plate, fuel/matrix interactions can impact the overall fuel plate performance. To continue the investigation of the irradiation performance of Si-rich fuel/matrix interaction layers, RERTR-6 fuel plate V1R010 (U-10Mo/6061 Al) was characterized using scanning electron microscopy. This fuel plate was of particular interest because of its similarities to fuel plate R1R010, which had U-7Mo particles dispersed in 6061 Al. Both fuel plates were irradiated as part of the RERTR-6 experiment and saw very similar irradiation conditions. R1R010 was characterized in another study and was observed to form relatively uniform Si-rich layers during fabrication that remained stable during irradiation. Since U-10Mo does not interact as much with 6061 Al at high temperatures to form layers, it was of interest to characterize a fuel plate with these particles since it would allow for a comparison of fuel plates with different amounts of pre-irradiation interaction zone formation, which were then exposed to similar irradiation conditions. This paper demonstrates how the lower amount of interaction layer development in V1R010 during fabrication appears to impact the overall performance of the fuel plate, such that it does not behave as well as R1R010 in terms of interaction layer stability. Additionally, the results of this study are applied to improve the understanding of fuel/cladding interactions in monolithic fuel plates that consist of U-10Mo foils encased in 6061 Al cladding.

1. Introduction

It has been observed that during irradiation of a fuel plate the interaction between U-7Mo particles and the Al matrix can impact the performance of a fuel plate by producing

interaction zones that may not exhibit favorable irradiation performance [1,2]. In some cases, fission gases will migrate through the layer to the interaction layer/matrix interface where relatively large pores can develop. These pores, in turn, can eventually linkup, resulting in eventual fuel plate failure. It has been suggested that the addition of Si to the matrix of a dispersion fuel can alter the phases that typically develop in the interaction zone of a U-Mo fuel with Al matrix such that the more Al-rich phases will not form [3,4]. The result would be a more stable interaction product since phases like UAl_3 have been observed to be stable. In fact, irradiated dispersion fuel plates with Si added to the matrix have exhibited improved performance [5-7]. Potentially, the production of Si-rich interaction layers around the fuel particles during fabrication may play a role in the improved performance that has been observed for dispersion fuel with Si-containing matrix [8].

To continue the investigation of how fuel/matrix interactions affect fuel performance, RERTR-6 fuel plate V1R010 (U-10Mo/6061 Al) was characterized using scanning electron microscopy (SEM). This fuel plate was of particular interest because of its similarities to fuel plate R1R010, which had U-7Mo particles and 6061 Al matrix and was also irradiated in the RERTR-6 experiment. R1R010 was observed to form relatively uniform Si-rich layers during fabrication that remained stable during irradiation, which resulted in good overall irradiation performance of the fuel plate [9]. On the other hand, U-10Mo, which does not interact with 6061 Al to the extent U-7Mo does during high temperature fabrication processes [10,11], was of interest for characterization because it would allow for a comparison of fuel plates with different amounts of pre-irradiation interaction zone formation that were exposed to similar irradiation conditions. This paper demonstrates how the lower amount of interaction layer development in V1R010 during fabrication appears to have impacted the overall performance of the fuel plate, such that it did not behave as well as R1R010.

Another benefit to the SEM analysis of V1R010 was that the results generated could be used to shed light on the fuel foil/cladding interaction in irradiated monolithic fuel plates that were fabricated using U-10Mo fuel and 6061 Al cladding. Comments are made about the growth and change in Si content of these layers during irradiation.

2. Experimental

SEM analysis, combined with energy-dispersive and wavelength-dispersive spectroscopy (EDS/WDS), was first performed on a cross-section of archive fuel plate V1R030 to determine the starting microstructure of a fuel plate with U-10Mo particles dispersed in 6061 Al after fabrication and before being inserted into the RERTR-6 experiment. Then, the same analysis was performed on a one-mm-diameter punching taken from the low-flux and high-flux side of irradiated fuel plate V1R010. This fuel plate sat edge-on to the core during irradiation, which resulted in the neutron flux gradient across the width of the fuel plate. It has been over three years since this plate was discharged from the Advanced Test Reactor (ATR), and so it could be handled in the Electron Microscopy Laboratory (EML). The punching microstructures were characterized, and compositional analysis was performed to determine the partitioning behavior of the fuel, cladding, and

fission product constituents between the fuel phases during irradiation.

3. SEM Results

3.1 Archive Sample V1R030

In Fig. 1, backscattered electron images of some fuel particles in V1R030 are presented. No fuel/matrix interaction layers around the fuel particles can readily be observed. WDS X-ray mapping for Mo indicated that the grain boundary regions were depleted in Mo. Point-to-point compositional analysis indicated that the mean Mo concentration in what appeared to be phases at the grain boundaries was 7.4 wt% ($\sigma = 0.4$), and internal to the grains the mean Mo concentration was 11.9 wt% ($\sigma = 0.5$). WDS X-ray mapping showed that Si-rich layers were present around the fuel particles (see Fig. 2). These thin layers could be resolved in high magnification images (see Fig. 3). Point-to-point compositional analysis confirmed the observation that the interaction layers were Si-rich. Due to the narrow thickness of the interaction layers, the results of compositional analysis were very qualitative. Overall, the thickness of the interaction layer was estimated to be in the tenths-of-a-micron range.

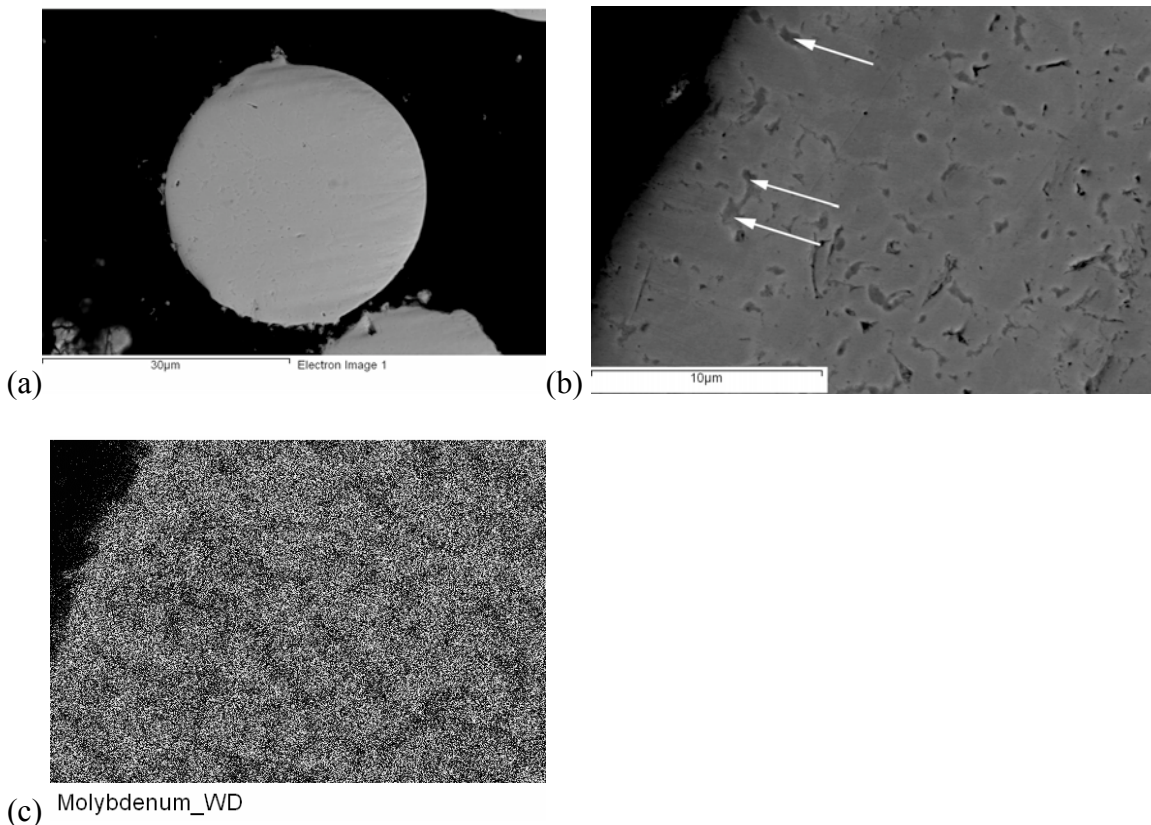


Fig. 1. Backscattered electron images (a,b) of the microstructure observed for the U-10Mo particles in as-fabricated RERTR-6 fuel plate V1R030, and (c) a WDS Mo X-ray map performed for the region shown in (b). The arrows in (b) identify some of the grain boundary phases that were compositionally analyzed.

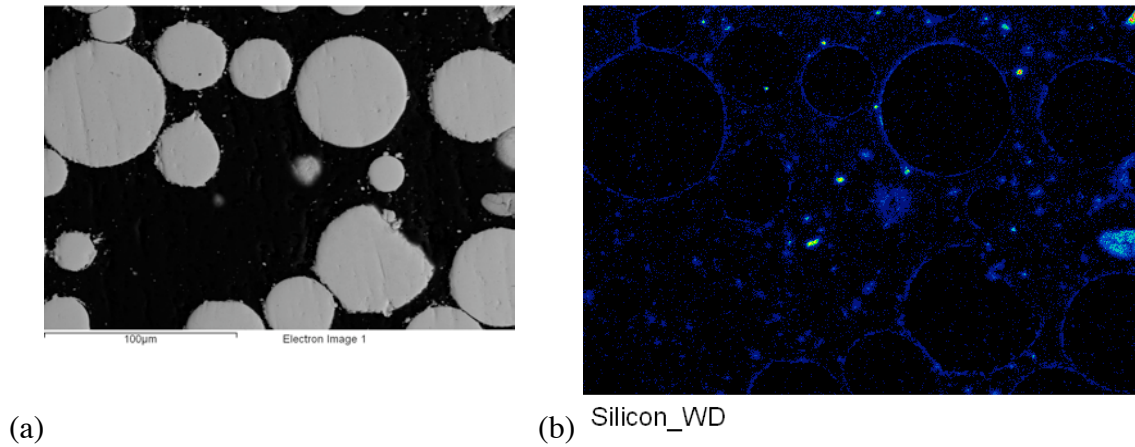


Fig. 2. Backscattered electron image (a) and WDS Si X-ray map (b) for fuel plate V1R030.

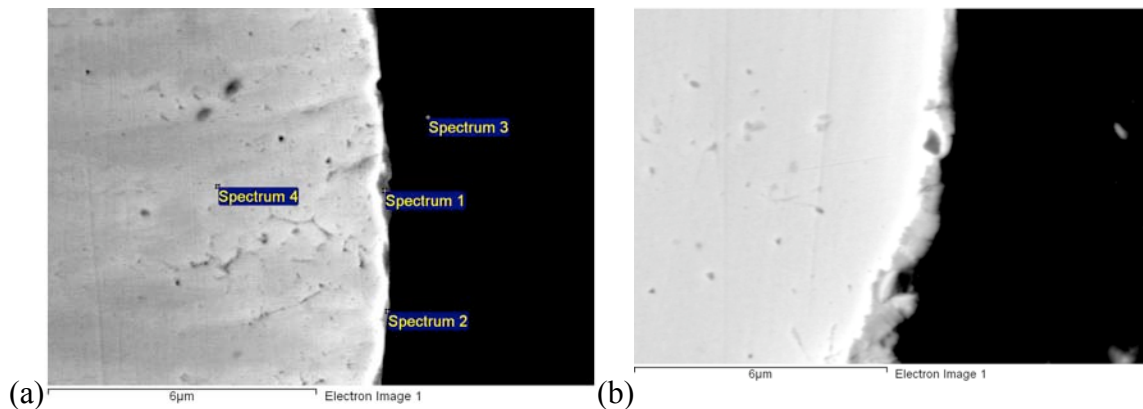


Fig. 3. Backscattered electron images of the narrow fuel/matrix interaction layer in fuel plate V1R030.

3.2 Low-Flux Punching from V1R010

For the irradiated fuel plate V1R010, a backscattered electron image of the microstructure observed on the low-flux side of the fuel plate is presented in Fig. 4. Uniform interaction layers can be identified around the U-10Mo fuel particles. In Fig. 5 are presented WDS X-ray maps for U, Mo, Al, Si, and Mg, and they show that negligible Si or Mg is observed in the interaction layers. Si is primarily contained in precipitates in the fuel meat matrix. Since this layer is thicker than for the case of the as-fabricated sample, the EDS compositional analysis results are more reliable. In general, it was confirmed that negligible Si and Mg were present in the interaction layer. The Al/(U+Mo) of the layer was near 4. Image analysis was performed on the SEM images of the microstructure of the low-flux punching from V1R010. It was determined the average interaction layer thickness around the fuel particles was $2.7 \mu\text{m} \pm 0.6$.

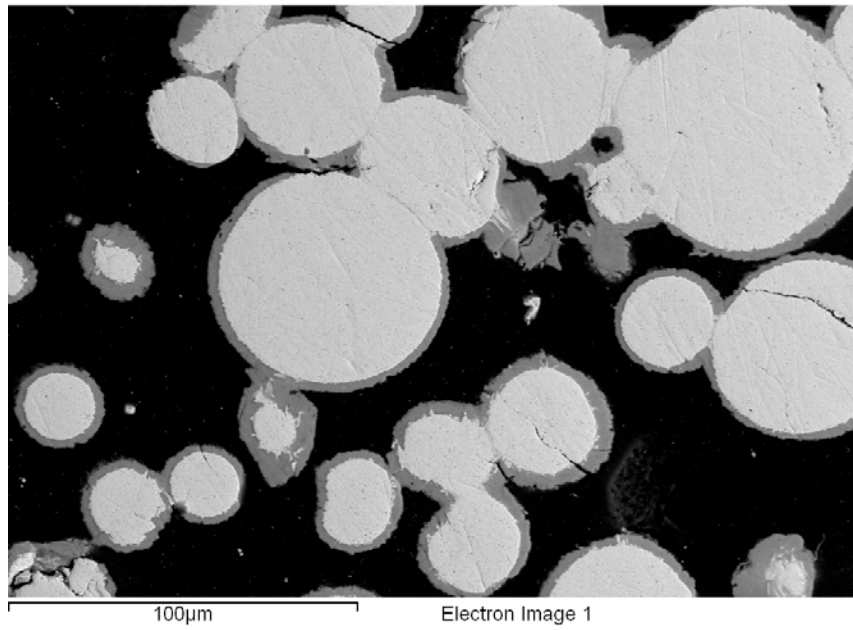
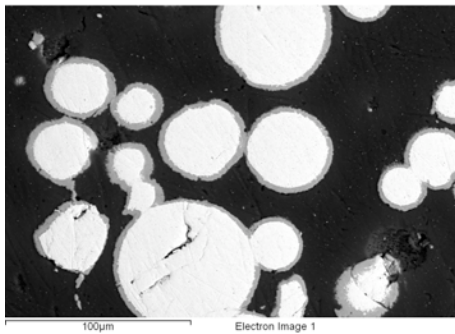
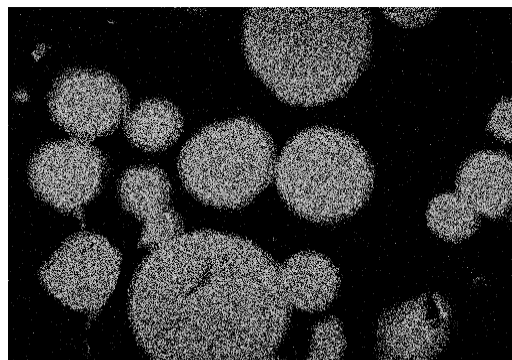


Fig. 4. Backscattered electron image of the microstructure observed at the low-flux side of VIR010.



(a)



(b) Uranium_WD

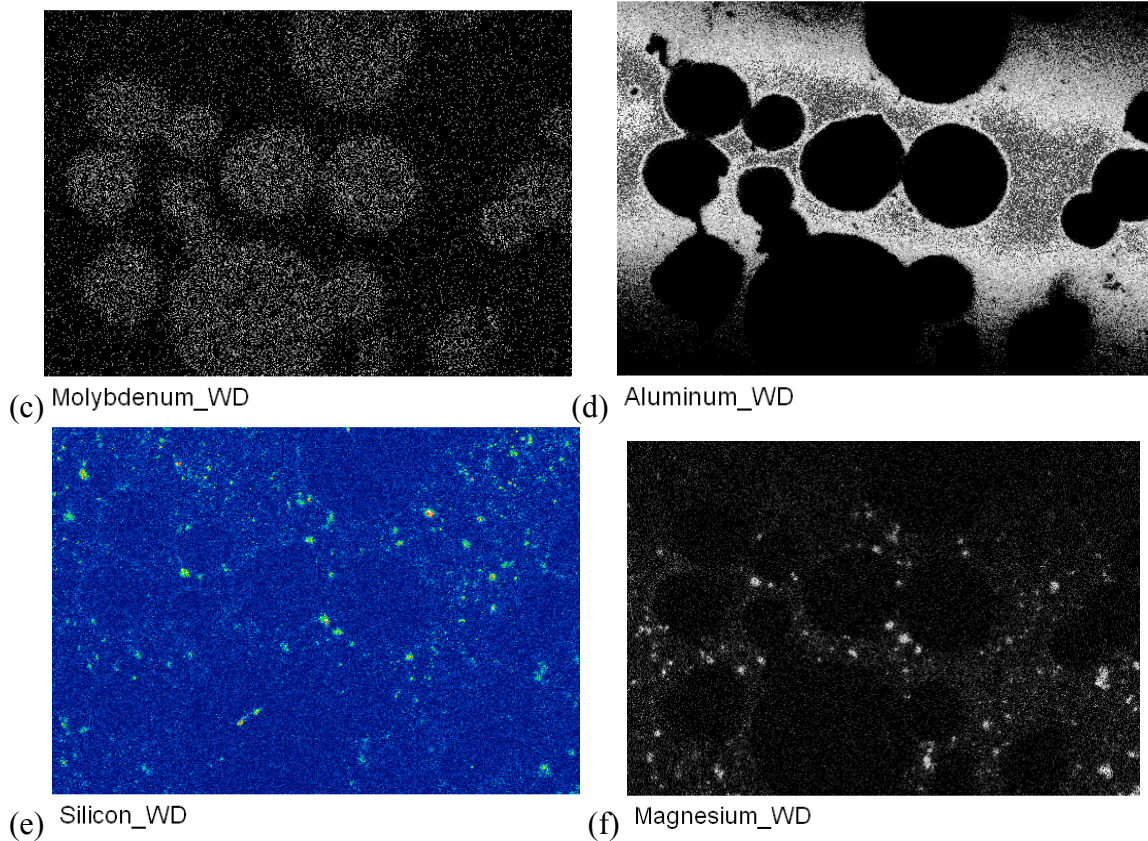


Fig. 5. Backscattered electron image (a) and WDS X-ray maps for (b) U, (c) Mo, (d) Al, (e) Si, and (f) Mg taken for the low-flux punching.

3.3 High-Flux Punching from V1R010

On the high-flux side of V1R010, thicker fuel/matrix interaction layers were observed (see Fig. 6). WDS X-ray mapping (Fig. 7) showed negligible Si in the interaction layers, and EDS point-to-point compositional analysis performed on interaction layers confirmed this result. The Al/(U+Mo) ratio of the layer was near 4. Image analysis was performed on the SEM images of the microstructure of the low-flux punching from V1R010. It was determined that the average interaction layer thickness around the fuel particles was $6.2 \mu\text{m} \pm 0.9$.

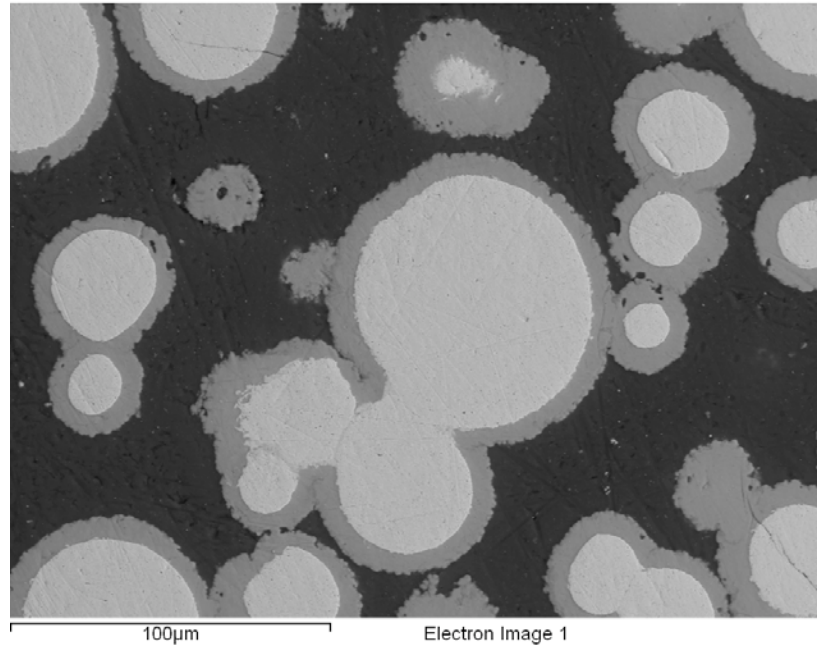


Fig 6. Backscattered electron image of the microstructure observed at the high-flux side of V1R010.

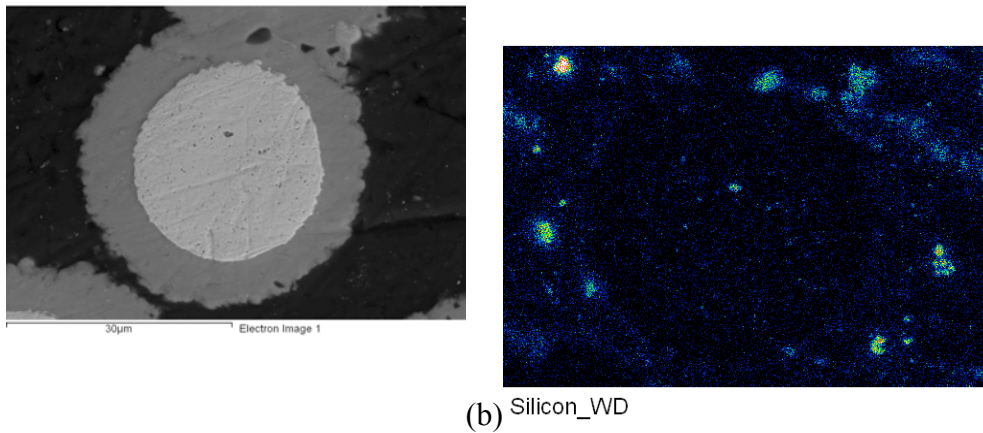


Fig. 7. Backscattered electron image (a) and Si WDS X-ray map (b) for the high-flux punching. The enriched Si areas are the Si precipitates in the 6061 Al.

4. Discussion

Based on the SEM analysis of fuel plate V1R010 and the archive fuel plate V1R030, irradiation to the conditions of the RERTR-6 experiment changes the starting, as-fabricated microstructure of a fuel plate with U-10Mo particles dispersed in 6061 Al. Around the fuel particles, the original thin, Si-rich interaction layers, which were tenths-of-a-micron thick after fabrication, grew to $2.7 \mu\text{m} \pm 0.6$ in thickness on the low-flux side

of the plate and to a thickness of $6.2 \mu\text{m} \pm 0.9$ on the high-flux side.

The observed interaction layer behavior described above for V1R010 is markedly different than what was observed for fuel plate R1R010 [8], which was irradiated under similar conditions in the RERTR-6 experiment (see Table 1), and had the same matrix but different fuel particles (U-7Mo). V1R010 was exposed to a slightly higher temperature and heat flux, but the fission density and fission rate values were almost identical. After fabrication, fuel plates with U-7Mo and Al-Si alloy matrices contain Si-rich interaction layers that are thicker than the tenths-of-a-micron-thick layers observed for V1R030 [12]. During irradiation of R1R010, these thicker, Si-rich layers did not change much in composition or thickness. A backscattered electron image and Si X-ray map from the low-flux side of R1R010 are presented in Fig. 8. Analogous Si X-ray maps were observed for the sample from the high-flux side of R1R010.

Table 1. Comparison of the calculated values for peak temperature, fission density, fission rate, and peak heat flux for punchings from the low and high-flux sides of R1R010 and V1R010.

Sample Label	Calculated Peak Punching Temperature ($^{\circ}\text{C}$)	Local Fission Density (10^{21} fcm^{-3})	Ave. Fiss. Rate ($10^{14} \text{ fcm}^{-3}\text{s}^{-1}$)	Peak Heat Flux for entire Punching (W/cm^2)
R1R010 (low-flux)	87	2.2	1.9	90
V1R010 (low-flux)	100	2.3	2.0	100
R1R010 (high-flux)	102	3.3	2.9	140
V1R010 (high-flux)	115	3.4	2.9	150

Image analysis showed that on the low-flux side of R1R010 the interaction layer thickness was $1.5 \mu\text{m} \pm 0.6$, and on the high-flux side the thickness was $2.8 \mu\text{m} \pm 0.6$. These thicknesses are about half of what was observed for V1R010. Fig. 9 compares the R1R010 and V1R010 microstructures on the low and high-flux sides of the fuel plates, and shows the increased interaction layer thicknesses in V1R010. The optical micrographs show how particularly on the high-flux side of the fuel plate, V1R010 developed a microstructure markedly different from the one observed for R1R010. This microstructure exhibited much thicker interaction layers. The differences in microstructure seem to indicate a difference in the irradiation behavior of the interaction layers for R1R010 compared to V1R010. Basically, the layers in R1R010 behaved the best (i.e., remained relatively thin and Si-rich), while the V1R010 layers grew in thickness, with the thickest layers observed on the high-flux side of the fuel plate. Since after irradiation the V1R010 layers were deficient in Si and the layers in R1R010 were enriched in Si, the better performance for R1R010 could be attributed to the fact that the

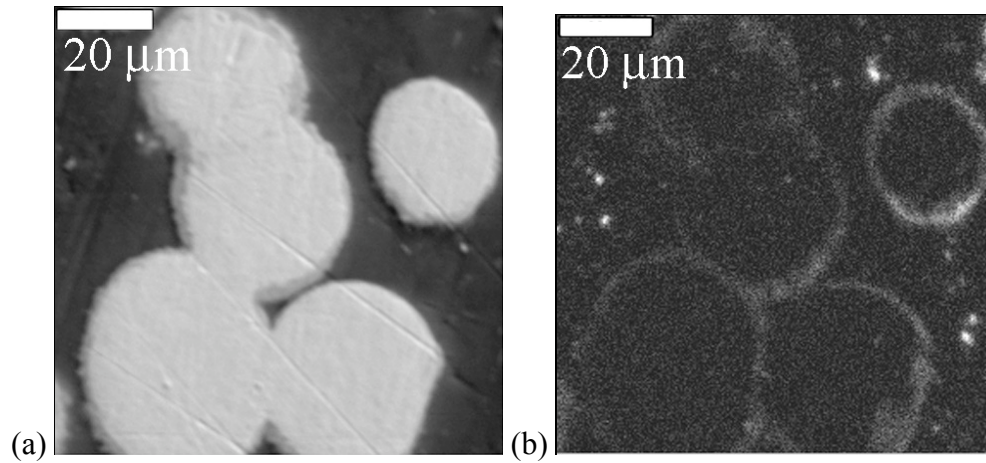


Fig. 8. Backscattered electron image (a) and Si WDS X-ray map (b) for the punching from the low-flux side of fuel plate R1R010. Si-rich precipitates are present in the 6061 Al matrix.

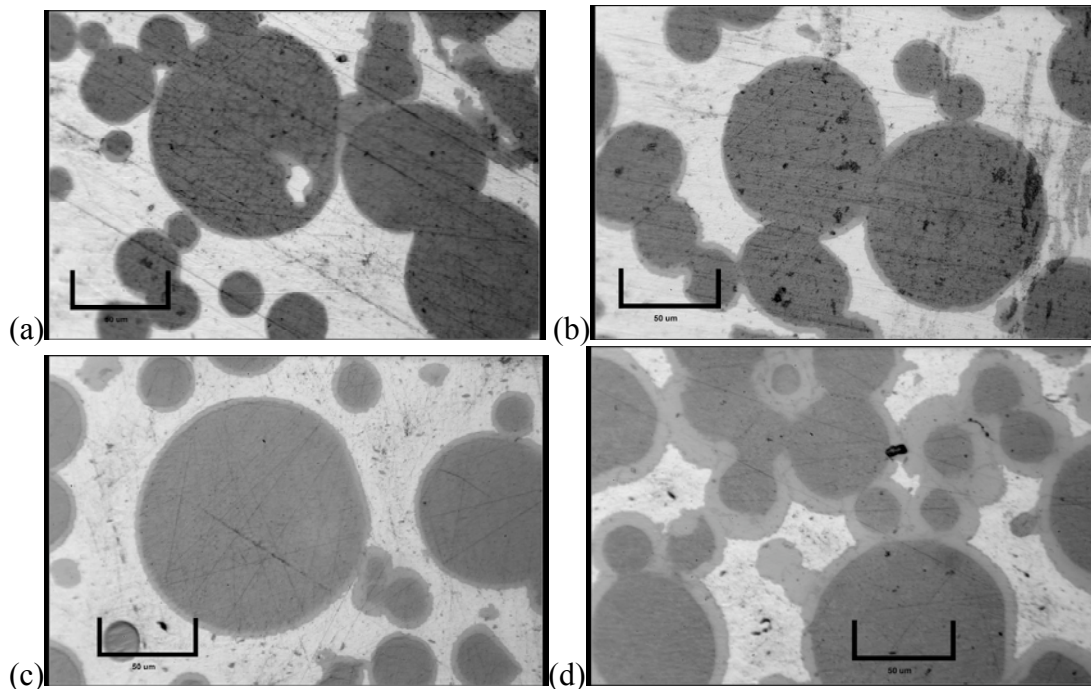


Fig 9. Optical micrographs of the microstructures observed on the low-flux (a) and high-flux (b) side of fuel plate R1R010 (U-7Mo/6061 Al) and (c) the low-flux and (d) the high-flux side of fuel plate V1R010 (U-10Mo/6061 Al). The micron bar is 50 μm .

original as-fabricated layers remained thin and enriched in Si. This suggests that if the original Si-rich layers are of significant thickness in an as-fabricated fuel plate, then they can survive irradiation to RERTR-6 conditions and will remain relatively thin and Si enriched. On the other hand, if the layers are too thin in an as-fabricated fuel plate, then they will grow in thickness and become depleted in Si.

Besides just improving the understanding of fuel/matrix interaction layer behavior during irradiation of dispersion fuels, another benefit of the characterization of fuel plate VIR010 is the fact that the developed interaction layers for this plate should be similar to ones that can develop in an irradiated monolithic fuel plate with a U-10Mo foil and 6061 Al cladding, particularly for plates that begin irradiation with little foil/cladding interaction layer formation. For HIPed U-10Mo fuel plates, the exposure to up to 580°C temperatures will result in the presence of up to 2 to 3 microns of interaction layer thickness at the U-10Mo/6061 Al interface after fabrication [11]. Like for dispersion fuel plates, there are different reaction rates with 6061 Al in monolithic fuel plates, depending on the Mo content in the fuel. U-10Mo reacts much more sluggishly than does U-7Mo. In fuel plates HIPed at 580°C, the U-7Mo foil is almost completely consumed by interaction product (see Fig. 9), and the U-10Mo foil reacts little with the 6061 Al cladding to form an interaction product. However the interaction that does occur for U-10Mo versus 6061 Al at 580°C is greater than what is seen for dispersion fuels rolled at 500°C.

For RERTR-6 monolithic fuel plates, some regions of the interaction layer that formed during irradiation developed porosity [13]. Since high temperature interactions between U-10Mo and 6061 Al in a monolithic fuel plate do not always produce uniform Si-rich layers along the foil/cladding interface [10], those areas along the U-10Mo/6061 Al interface where uniform layers are not produced will not exhibit good irradiation behavior. Based on the characterization performed on VIR010, significant interaction layer growth can occur between U-10Mo and 6061 Al during irradiation when a Si-rich interaction layer is not already present, and the developed layer is found to contain negligible Si. Within this layer, fission gas bubbles can develop that may impact the bond integrity of the foil/cladding interface. For monolithic fuel plates where a Zr diffusion barrier is placed between the U-10Mo and the 6061 Al cladding, the deleterious formation of U-10Mo/6061 Al interaction layer will be eliminated.

5. Conclusions

Based on the SEM characterization of irradiated dispersion fuel plate VIR010 followed by a comparison of the results with those produced for irradiated dispersion fuel plate R1R010, it can be concluded that the morphology of the interaction layers present after fabrication of a fuel plate can impact the fuel plate's performance during irradiation. For a fuel plate with 6061 Al matrix and Si-rich interaction layers that are only tenths-of-a-micron thick, the performance of the fuel plate will most likely not be as good as one that starts with Si-rich interaction layers that are thicker (1 to 2 μm thick). The thinner as-fabricated Si-rich interaction layers will become Si deficient and will grow in thickness during irradiation, while the thicker as-fabricated Si-rich layers will not change much in thickness and will remain Si-rich even up to relatively high burnups. Since layer stability should also depend on the amount of Si in the matrix that is available to diffuse to the interaction layer during irradiation, the differences in Si-rich interaction layer behavior for U-7Mo fuels compared to U-10Mo, as described in this paper, could be different for a fuel with a matrix with more or less Si than 6061 Al.

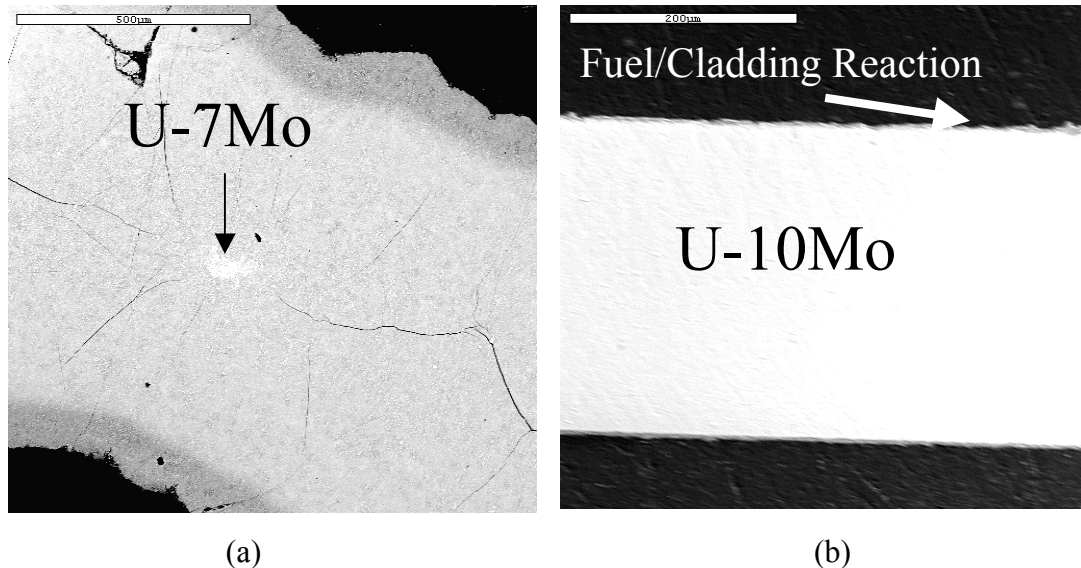


Fig 9. SEM micrographs of (a) U-7Mo and (b) U-10Mo foils after HIPing at 580°C for 3 hrs. The black areas are 6061 Al cladding and the medium-contrast areas are interaction product [5]. Micron bar is 500 μm in (a), and 200 μm in (b).

For HIPed monolithic fuel plates that consist of a U-10Mo foil and 6061 Al cladding, there is a good chance that there will be locations along the U-10Mo/6061 Al interface where the interaction layers that develop during irradiation are not enriched in Si and may contain regions of fission gas porosity. In order to eliminate the deleterious effects of such a layer on the bonding between a fuel foil and the cladding, it will be beneficial to introduce a diffusion barrier layer that will keep such a layer from developing.

Acknowledgments

This work was supported by the U.S. Department of Energy, Office of Nuclear Materials Threat Reduction (NA-212), National Nuclear Security Administration, under DOE-NE Idaho Operations Office Contract DE-AC07-05ID14517. Hot Fuel Examination Facility personnel are recognized for their contributions in destructively examining fuel plates, and Ashley Ewh is recognized for her assistance in performing image analysis.

References

- [1] A. Leenaers et al., J. Nucl. Mater. 335 (2004) 39-47.
- [2] G. L. Hofman et al., RERTR 2003 Chicago, IL, October 5-10, 2003.
- [3] W. C. Turber and R.J. Beaver, ORNL-2602, Oak Ridge National lab, 1959.
- [4] G. L. Hofman et al., RERTR 2004, Vienna, Austria, November 7-12, 2004.
- [5] G. L. Hofman et al. RERTR 2005, Cape Town, South Africa, Oct. 29-Nov.2, 2005.
- [6] S. Dubois et al., RRFM 2007, Lyon, France, March 11-15, 2007.
- [7] A. Leenaers et al., RRFM 2008, Hamburg, Germany, March 2-5, 2008.
- [8] D. D. Keiser, Jr. et al., GLOBAL 2009, Paris, France, Sep. 6-10, 2009.
- [9] D. D. Keiser, Jr. et al., J. Nucl. Mater. 393 (2009) 311-320.
- [10] D. D. Keiser, Jr., Defect and Diffusion, Vol. 266 (2007) pp. 131-148.
- [11] D. D. Keiser, Jr. et al., RRFM 2007, Lyon, France, March 11-15, 2007.
- [12] D. D. Keiser, Jr. et al., RERTR 2008, Washington, D. C., October 5-9, 2008.
- [13] D. D. Keiser, Jr. et al., RERTR 2007, Prague, Czech Republic, September 24-27, 2007.